

Finite temperature electronic structure of Diamond and Silicon

Vaishali Shah*

Interdisciplinary School of Scientific Computing, Savitribai Phule Pune University, Pune, 411007, India

Bhavik Sanghavi, Rahul Ramchandani, M. P. Gururajan and T. R. S. Prasanna†

Department of Metallurgical Engineering and Materials Science,
Indian Institute of Technology, Bombay, Powai, Mumbai - 400076, India

(Dated: February 21, 2018)

The electron-phonon interaction contribution to the electronic energies is included in density functional total energy calculations with *ab initio* pseudopotentials via the formalism of Allen [Phys. Rev. B, 18 5217 (1978)] to obtain the temperature dependent electronic structure of diamond and silicon. This method allows us to obtain the thermally-averaged *ab initio* electronic structure in a straightforward and computationally inexpensive way. Our investigations on the finite temperature electronic structure of diamond and silicon bring out that a new criterion, that of temperature transferability, is required in the input *ab initio* pseudopotentials for temperature dependent studies. The temperature transferability of the Troullier-Martins pseudopotentials used in this work is strongly dependent on the cut-off radius and the inclusion of the unbound 3d⁰ state. The finite temperature indirect band gaps are highly sensitive to the choice of cut-off radius used in the pseudopotentials. The finite temperature band structures and density of states show that thermal vibrations affect the electron energies throughout the valence and conduction band. We compare our results on the band gap shifts with that due to the Debye-Waller term in the Allen-Heine theory and discuss the observed differences in the zero point and high temperature band gap shifts. Although, the electron energy shifts in the highest occupied valence band and lowest unoccupied conduction band enable to obtain the changes in the indirect and direct band gaps at finite temperatures, the shifts in other electronic levels with temperature enable investigations into the finite temperature valence charge distribution in the bonding region. Thus, we demonstrate that the Allen theory provides a simple and theoretically justified formalism to obtain finite temperature valence electron charge densities that go beyond the rigid pseudo-atom approximation.

I. INTRODUCTION

Most electronic structure studies are performed for static lattices that are implicitly assumed to be at 0 K. Experimental investigations and determination of material properties are however performed at finite temperatures. The two important effects of temperature on the material are the lattice expansion and lattice dynamics. The effect of the lattice expansion on electronic energies is straightforward to obtain. However, the electron-phonon interaction which has a major contribution from the lattice dynamical behaviour is harder to calculate. Temperature affects the nuclear motion in materials leading to lattice dynamics which alters the electronic energies by $2\text{--}4\text{ k}_B\text{T}^{1\text{--}3}$ in solids. The resistivity of metals, directional Compton profiles, infrared, Raman, optical spectra, specific heats, heat conduction, band gaps etc. are affected by the electron-phonon interaction. In order to compare the results of experiments with the theoretical simulations the effect of electron-phonon interaction needs to be included in the calculations of these phenomena.^{2–4}

Although of significant importance, the electron-phonon interaction happens to be the most difficult

to compute from first principles. Currently, there are three major approaches⁵, namely, the molecular dynamics method, the frozen phonon method and the perturbation theory method to understand the effects of the electron-phonon interaction on material properties. Each of these approaches has its advantages and disadvantages^{4,5}. The to-date developments to include the electron-phonon interactions in *ab initio* calculations and their computational implementations is discussed in detail in a rigorous and elegant review by Giustino⁴.

In the context of temperature dependent semiconductor band gaps, the earliest attempt to include the electron-phonon interaction was by Fan⁶ who calculated the self-energy (SE) contribution to the semiconductor band gap shifts. This term is also referred to as the Midgal term in superconductor literature⁴. Soon afterwards, Antoncik⁷ calculated the Debye-Waller (DW) correction to the semiconductor band gaps. Subsequently, several authors calculated the semiconductor band gap shifts due to thermal vibrations, mostly by incorporating the Debye-Waller term^{8–12}. These investigations led Baumann¹³ to suggest that both self-energy and DW corrections are necessary for a complete account of the role of thermal vibrations on electron energies.

Allen and Heine¹ developed the formal basis for incorporating electron-phonon interactions in the harmonic approximation at constant volume using second-order perturbation theory. In this formalism¹, the DW term and the SE term appear separately and the total electron

* vaishali@unipune.ac.in

†Corresponding author: prasanna@iitb.ac.in

energy shift is a sum of the two terms. The implementation of the formalism requires a concurrent calculation of the DW and SE term. The calculation of the DW term is approximated by a second order expansion with the neglect of the higher order terms. Further, by exploiting translational invariance the DW term (in the second order form) and the SE term is recast¹ to have similar forms. All recent studies based on the Allen-Heine theory use the recasted DW term since calculating it directly in the second order form is computationally complex.

The Allen-Heine theory was earlier used with empirical pseudopotentials to obtain the band gap shifts in semiconductors^{14,15}. However, in the last decade, several *ab initio* studies^{16–24} based on it have been reported. These studies report the band gap shifts at specific k points that usually correspond to the indirect and direct band gaps^{16–24}. In these studies, the band gaps at all high symmetry points or the complete valence electron band structure along the symmetry lines in the Brillouin zone have not been reported.

Subsequent to the Allen-Heine theory¹, a more accurate theory was developed by Allen² for the temperature dependent band structure. In this theory, the DW term is considered to all orders instead of its truncated second order expansion as in the Allen-Heine theory. In the implementation of the Allen theory² with pseudopotentials, the first step is to correct the pseudopotential form factor with the DW term and use this corrected pseudopotential to obtain the finite temperature electronic structure. The second step is to calculate the SE term using the wavefunctions and energies obtained from the DW corrected electronic structure.

The Allen theory² provided the theoretical justification for the earlier empirical studies^{8–12} that calculated the finite temperature band gaps based on the DW correction step. It must be noted that the first step, the DW correction step, directly leads to the temperature dependent band structure. The band gap shifts obtained from the first DW correction step gave satisfactory band gap shifts in some cases and unsatisfactory results in other cases^{8–12}. The DW corrected empirical studies on the temperature dependence of band gaps in PbSe and PbTe, while giving reasonable results for the direct gap, failed to correctly estimate the indirect gap¹¹. Allen and Heine¹ and Allen² discuss this aspect and show that for accurate values of the finite temperature electron energies and band gap shifts the contribution from the SE term needs to be included, in general.

The second order Allen-Heine formalism¹ continues to be of interest and has been used in several recent *ab initio* calculation based studies^{16–24} to obtain the semiconductor band gap shifts with temperature. In contrast, the Allen theory² has not been used in *ab initio* studies, even though it is a more accurate approach¹ compared to the Allen-Heine theory.

In this article we demonstrate that the Allen theory can be combined with *ab initio* pseudopotentials to obtain *ab initio* finite temperature electronic structures

without any additional increase in the computational complexity of these calculations. We investigate the finite temperature electronic structure of diamond and silicon using the *ab initio* pseudopotential implementation of the Allen theory. We then compare the results of our theoretical calculations with earlier *ab initio* studies on diamond and silicon based on the second-order Allen-Heine theory.

The focus of this paper is to address the main issues that affect the implementation of the Allen theory² using *ab initio* pseudopotentials. Thus, only the DW contribution, which is the first step in Allen theory, has been calculated. The (Fan/Fan-Migdal) self-energy term, that is to be calculated from the results of the DW step, has not been evaluated.

However, calculation of the DW correction to the electronic energies is important for three reasons, as will be seen in this study. Firstly, the DW step is sufficient to address the fundamental question, viz. the viability of implementing Allen theory with *ab initio* pseudopotentials. Secondly, only the DW term can be the basis for the comparison of the Allen and Allen-Heine theories. And, thirdly, the DW step is sufficient to obtain finite temperature valence electron charge densities. Thus, the results of the present study have important implications for *ab initio* finite temperature electronic structure studies.

In the next section, we briefly describe the theory of Allen² for the inclusion of the electron-phonon interaction and its implementation within the pseudopotential method for band structure calculations. In Sec. III, we describe the computational implementation and give the details of our calculations of temperature dependent electronic structure. Sec. IV discusses the results of the temperature dependent band gap trends that were obtained using existing pseudopotentials and the need to use temperature transferable pseudopotentials in electronic structure calculations that are to be used to study the finite temperature properties. Our results on the temperature dependent band gap trends, band gap shifts at zero point vibration and higher temperatures for diamond (Sec. IV B) and silicon (Sec. IV C) are discussed in detail with implications. In the Sec. IV E, we show that theoretically it is possible to obtain charge densities that go beyond the rigid pseudo-atom approximation for a direct comparison with experimental data and this is then followed by conclusions in Sec. V

II. ALLEN'S THEORY AND ITS IMPLEMENTATION

In the theory of temperature dependence of the energy bands given by Allen-Heine¹ and Allen², a lattice of identical atoms is considered with the atoms undergoing a small thermal displacement \mathbf{u}_α about their equilibrium positions α . In this system, the potential experienced by an electron due to phonon disorder is assumed to move rigidly with the atoms so that the perturbation to the system can be expressed as

$$H_{e-p} = \sum_l [V(\mathbf{r} - \mathbf{R}_\alpha) - V(\mathbf{r} - \alpha)] \quad (1)$$

where, $V(\mathbf{r})$ is the atomic potential, \mathbf{R}_α is the displaced position of the atom, α is the equilibrium position and $\mathbf{u}_\alpha = \mathbf{R}_\alpha - \alpha$ is the displacement. The thermal displacements of atoms are time dependent and are related to the phonon frequency. The perturbed electron energy can be calculated in the adiabatic approximation by a second order Taylor expansion of Eq. 1 as proposed by Allen-Heine¹, where the first two terms are

$$H_{e-p}^{(1)} = \sum_l \left[\frac{\partial V(r - \alpha)}{\partial r_n} \right] u_{\alpha n} \quad (2)$$

$$H_{e-p}^{(2)} = \frac{1}{2} \sum_l \left[\frac{\partial^2 V(r - \alpha)}{\partial r_n \partial r_m} \right] u_{\alpha n} u_{\alpha m} \quad (3)$$

Considering the thermal average $\langle H_{e-p} \rangle$, the only non-vanishing terms are the even powered terms like Eq. 3 in the Taylor expansion. The thermal average of Eq. 3 is the self energy correction in a Bloch-wave basis set. However, in a plane wave basis set all the non-vanishing terms can be considered and result in the Debye-Waller corrections to the crystal potential and Eq. 1 can be rewritten as

$$H_{e-p} = \sum_{\mathbf{k}\mathbf{k}'} V(\mathbf{k}' - \mathbf{k}) s(\mathbf{k}' - \mathbf{k}) c_{\mathbf{k}'}^\dagger c_{\mathbf{k}} \quad (4)$$

In this equation the \mathbf{k}, \mathbf{k}' span all the Brillouin zones and s is the structure factor. The thermal average of the perturbed Hamiltonian in reciprocal space is

$$\langle H_{e-p} \rangle = \sum_{\mathbf{k}} \sum_{\mathbf{G}\mathbf{G}'}^{BZ} V(\mathbf{G}' - \mathbf{G}) (e^{-W(\mathbf{G}' - \mathbf{G})} - 1) c_{\mathbf{k} + \mathbf{G}'}^\dagger c_{\mathbf{k} + \mathbf{G}} \quad (5)$$

This Hamiltonian is periodic and the calculation in Fourier space requires the sum to be performed only on the first Brillouin zone. When added to the unperturbed Hamiltonian it leads to a reduction of the pseudopotential form factors $V(\mathbf{G})$ of the static lattice by DW factors $e^{-W(\mathbf{G})}$ to incorporate the effect of the DW term of the electron-phonon interaction. This result of Allen² provided the theoretical basis for the earlier empirical studies⁸⁻¹² and is also the theoretical basis for the present *ab initio* study.

The underlying assumptions in both the Allen-Heine¹ and Allen² theories are the adiabatic approximation and the rigid atom approximation. The *ab initio* pseudopotentials are generated under the assumption of frozen-core approximation for the core electrons, which satisfies the rigid-atom approximation. Thus, Allen-Heine¹ and Allen² theories are valid for semiconductors and insulators at all temperatures. The adiabatic approximation

condition, however, breaks down for metals at low temperatures since the self-energy term cannot be correctly represented¹⁻³.

From Eq. 5, the finite temperature pseudopotential form factor for any ion can be written as

$$V_i^{ps}(\mathbf{G}, T) = V_i^{ps}(\mathbf{G}, 0) e^{-W_i(\mathbf{G}, T)} \quad (6)$$

where the DW factor^{8,10,25} is given by, $W_i = \frac{\langle u_i^2 \rangle |G|^2}{2}$ and $\langle u_i^2 \rangle$ is the mean square displacement of atom i .

In order to use Eq. 6 in *ab initio* studies, both the pseudopotential form factor, $V(\mathbf{G})$ and the DW factor (W) need to be obtained from *ab initio* studies. Currently, there are several *ab initio* methods²⁶⁻³³ to calculate DW factor from first principles. In these studies, *ab initio* DW factor has already been calculated for several materials including many semiconductors.

However, if necessary, even experimental DWF can be used in Eq. 6. We note that in several *ab initio* studies^{28,29,34} experimental lattice parameters are used. In particular, Erba et. al²⁸ provide the justification for the use of experimental lattice parameters viz. that they can be validated by separate *ab initio* studies. Therefore, if necessary, the same justification can be the basis for the use of experimental DWF in *ab initio* studies based on Allen theory.

The other requirement is that of *ab initio* pseudopotentials which can be used in Eq. 6 to obtain finite temperature band structure. As discussed in Sec.IV, this is a much more stringent condition than expected.

It is of interest to compare both the zero-point and the higher temperature band gap shifts obtained using the Allen and Allen-Heine theories since the latter uses the second-order approximation to the DW term. In both, Allen and Allen-Heine theories, the band gap shifts should increase with temperature due to the increase in the mean-square displacements or W . The main difference in their formalism is that, in the Allen-Heine theory, the pseudopotential form factor $V_G e^{-W}$ is approximated¹ by $V_G (1-W)$ neglecting higher order terms in the expansion. The band gaps obtained by the DW corrected pseudopotentials, $V_G e^{-W}$ in the Allen theory and $V_G (1-W)$ in the Allen-Heine theory, are to be compared with the band gaps obtained with the static lattice pseudopotential form factor, V_G , to obtain the finite temperature band gap shifts.

We can examine the effect of the second-order approximation used in the Allen-Heine theory. For higher values of the mean square displacement, the pseudopotential form factor in the Allen-Heine theory, $V_G (1-W)$, is smaller than that of the actual value, $V_G e^{-W}$, that is used in the Allen theory. This implies that the pseudopotential form factor used in the Allen-Heine theory undergoes a larger amount of change from the static lattice value (V_G) than the pseudopotential form factor in the Allen theory. It follows that, at higher temperatures, the Allen-Heine theory should give larger band

gaps shifts than Allen theory due to the neglect of higher order terms.

In the Allen-Heine theory, the self-energy (SE) term contribution is calculated from the static lattice electron wavefunctions and energies. In contrast, in the Allen theory, the SE term contribution is to be calculated from the finite temperature electron wavefunctions and energies obtained from the DW correction step. Thus, the SE term contributions in the Allen and the Allen-Heine theories will be different.

Therefore, the primary basis for the comparison of the Allen-Heine and Allen theories is the Debye-Waller (DW) term contribution, which, in principle, must give identical band gap shifts for the same pseudopotential and same mean-square displacement values as long as the second-order approximation is valid.

III. COMPUTATIONAL METHODOLOGY

We have performed *ab initio* total energy calculations based on density functional theory to obtain the band structure of diamond and silicon at different temperatures using the Quantum Espresso (QE) software package³⁵. The equilibrium lattice constant for the static lattice (0 K) was obtained by choosing the energy converged k-point mesh and kinetic energy cutoff. A 6x6x6 k-point mesh and kinetic energy cutoff of 60 Ry for carbon (diamond) and 40 Ry for silicon was used in all our calculations.

To incorporate the effect of finite temperature on the electronic structure, we modified the QE code so that the local part of the *ab initio* atomic pseudopotential of the system under investigation is altered in G-space with the Debye-Waller factor, i.e. e^{-W} as in Eq. 6. The non-local part of the atomic pseudopotential is unmodified to preserve the angular dependence of the scattering potential as in the earlier work based on empirical pseudopotentials¹¹. With this alteration, the finite temperature pseudopotential form factor is obtained within the QE code for a given *ab initio* static lattice pseudopotential of any atom. Using a value of the mean square displacement $\langle u_i^2 \rangle$ appropriate for a chosen temperature, an electronic structure calculation was performed to obtain the band structure at that temperature.

All electronic structure calculations were performed for various temperatures up to 1000 K at constant volume using the equilibrium lattice constant obtained for the static lattice. The *ab initio* mean-square displacement $\langle u_i^2 \rangle$ values of C and Si listed in Table I at various temperatures were taken from the *ab initio* studies of Schowalter *et al.*²⁶. Using these values in the modified QE code, the self-consistent total energy and the band structure at different temperatures were obtained using different kinds of *ab initio* pseudopotentials.

T (K)	$\langle u_i^2 \rangle$ (\AA^2)	
	C	Si
0.001	0.001611	0.002471
100	0.001626	0.003196
200	0.00169	0.004865
300	0.001807	0.006788
400	0.001968	0.008772
600	0.002436	0.01287
800	0.002962	0.017022
1000	0.003529	0.021198

TABLE I: *Ab initio* mean-square displacement values for diamond and silicon at various temperatures²⁶.

IV. RESULTS AND DISCUSSION

We began our investigations on the effect of temperature on the electronic structure of diamond and silicon with several norm conserving pseudopotentials that are available in the pseudopotential library on the QE website³⁵. In addition, some optimized and ultrasoft pseudopotentials available on the QE website library, recently developed Optimized Norm Conserving Vanderbilt (ONCV) pseudopotentials³⁶, the GBRV pseudopotentials³⁷ and PAW pseudopotentials³⁸ were also investigated.

Separate electronic structure calculations were performed to obtain the band structure of diamond and silicon for each temperature up to 1000 K as given in Table I using each pseudopotential listed in Table II and III. The band gaps obtained for each pseudopotential were then compared across the range of temperatures used in this study. Table II and III list the trends in the band gaps obtained for diamond and silicon from our calculations. The equilibrium lattice parameter obtained for each pseudopotential is listed along with the experimental value for comparison.

For the static lattice case, almost all of the above pseudopotentials show excellent agreement in values of the indirect and direct band gaps reported in theoretical studies as all these pseudopotentials have hitherto been developed for static lattice *ab initio* calculations.

Several previous studies¹⁴⁻²³ on diamond and silicon, based on the Allen-Heine theory, using both *ab initio* and empirical pseudopotentials, have shown that the indirect and direct band gaps decrease with temperature in agreement with experiments. In particular, for diamond^{15,17,18} and silicon^{14,15}, the DW term alone leads to a decrease in the band gaps with temperature as calculated in the Allen-Heine theory.

Thus, the primary criterion that needs to be fulfilled when choosing *ab initio* pseudopotentials for temperature dependent studies on carbon (diamond) and silicon is that after modification with the DW factor, the direct and indirect band gaps must decrease with increasing temperatures. Only after this primary criteria is met

Pseudopotential (PP) Filename	a a.u.	Band gap (eV)			
		Static		Finite T trend	
		Indirect	Direct	Indirect	Direct
C.pbe-mt_gipaw	6.73	4.246	5.645	Decrease	Increase
C.pbe-n-kjpaw	6.74	4.135	5.599	Decrease	Increase
C.pbe-mt_fhi	6.63	4.308	5.756	Decrease	Increase
C.pw-mt_fhi	6.63	4.32	5.757	Decrease	Increase
C.blyp-mt	6.79	4.371	5.679	Decrease	Increase
C.blyp-hgh	6.79	4.317	5.664	Decrease	Increase
C.pbe-hgh	6.77	4.068	5.589	Decrease	Increase
C.pbe-van_bm	6.64	4.234	5.722	Decrease	Increase
C_pbe_v1.2.uspp.F	6.71	4.176	5.629	Decrease	Increase
C_ONCV_PBE-1.0	6.54	4.378	5.846	Decrease	Increase
Expt ²²	6.74	5.48	7.3	Decrease	Decrease

TABLE II: The indirect and direct band gap at 0 K and the trend in their values with increasing temperature (up to 1000 K) for the carbon (diamond) *ab initio* pseudopotentials. The names of the pseudopotential files are the same as in the source library with a .UPF extension

Pseudopotential (PP) Filename	a a.u.	Band gap (eV)			
		Static		Finite T trend	
		Indirect	Direct	Indirect	Direct
Si.pbe-mt_gipaw	10.31	0.633	2.572	Decrease	Decrease
Si.pbe-n-kjpaw	10.33	0.605	3.122	Increase	Decrease
Si.pbe-mt_fhi	10.33	0.614	2.561	Increase	Increase
Si.pw-mt_fhi	10.17	0.457	2.568	Increase	Increase
Si.blyp-hgh	10.41	0.905	2.849	Increase	Decrease
Si.pbe-n-van	10.34	0.614	3.108	Increase	Increase
Si.pbe-rrkj	10.35	0.639	2.558	Increase	Increase
Si_pbe_v1.uspp.F	10.33	0.691	2.533	Increase	Increase
Si_oncv_pbe-1.0	10.37	0.62	2.548	Increase	Dec-Inc
Si_oncv_pbe-1.1	10.35	0.60	2.546	Increase	Dec-Inc
Expt ²²	10.26	1.17	3.378	Decrease	Decrease

TABLE III: The indirect and direct band gap at 0 K and the trend in their values with increasing temperature (up to 1000 K) for the silicon *ab initio* pseudopotentials. The names of the pseudopotential files are the same as in the source library with a .UPF extension

can further finite temperature studies be performed. For example, the self-energy contributions should only be calculated for pseudopotentials which show the correct behaviour in the DW step.

We notice that, for diamond (Table II) all the pseudopotentials show decreasing indirect band gaps as is expected with increasing temperature. However, the direct band gaps are increasing with temperature which does not agree with the trends reported in literature. Thus, none of the *ab initio* pseudopotentials in Table II can be used for finite temperature electronic structure studies.

In the case of silicon only one pseudopotential, Si.pbe-mt_gipaw.UPF, gave the expected trend of decreasing

indirect and direct band gaps with increasing temperature. The lattice constant obtained with this pseudopotential also gives a better agreement with the experimental value. The calculated band gaps and the shifts in the band gaps for this Si pseudopotential, labelled $Si_{pbe-gipaw}$ in our study, are listed in Table IV.

Temp (K)	Band gap (eV)		Band gap shift (meV)	
	Indirect	Direct	Indirect	Direct
0	0.633	2.572		
0.001	0.539	2.544	94	28
100	0.512	2.537	121	35
200	0.449	2.519	184	53
300	0.376	2.494	257	78
400	0.296	2.466	337	106
600	0.136	2.396	497	176
800	-	2.319	-	253
1000	-	2.246	-	326

TABLE IV: The indirect and direct band gaps with temperature and the energy shifts in the direct and indirect band gaps for silicon obtained with Si.pbe-mt_gipaw.UPF ($Si_{pbe-gipaw}$) pseudopotential

It is well known that the Si band gaps are underestimated in the density functional calculations. A consequence of this underestimation is that at higher temperatures of 800 K and 1000 K the indirect band gap of Si is seen to vanish. As will be discussed in detail later (Sec IV C), while the band gap trends are correct, the actual values of the band gap shifts for the above pseudopotential, $Si_{pbe-gipaw}$, appear to be excessive when compared to literature values.

The finite temperature band gap results show that, in general, the *ab initio* pseudopotential developed for static lattice applications cannot be directly used for temperature dependent electronic structure calculations. The above results thus imply that for finite temperature studies, *ab initio* pseudopotentials need to be generated so as to satisfy an additional criterion, that of temperature transferability.

Since the *ab initio* pseudopotential is initially generated for static lattice conditions, it has to be generated with the usual criteria viz. the norm conservation criteria (present or absent) and the choice of the cut-off radius, r_c , to ensure the transferability of the pseudopotential to other chemical environments. The additional criterion of temperature transferability will ensure that the pseudopotentials can be used for finite temperature studies, in addition to static lattice calculations.

Semiconductors are the class of materials that are most suited to test for temperature transferability. This is because there is a stringent test of temperature transferability - the indirect and direct band gaps must exhibit the ‘‘Varshni effect’’ of redshift with increasing temperature³⁹. In addition, the band gap shifts must

be of the same order of magnitude when compared with existing experimental or theoretical results.

However, in some semiconductors the band gaps exhibit a blueshift with temperature^{4,11}. For such semiconductors, the temperature transferability criterion stands appropriately modified.

A. Pseudopotentials with temperature transferability

Considering that several of the currently available open source C and Si *ab initio* pseudopotentials (Table II and III) when used for finite temperature electronic structure calculations did not reproduce the correct band gap trends and band gap shifts, we generated pseudopotentials based on the Troullier-Martins method⁴⁰, with GGA/PBE⁴¹ and LDA/PZ^{42,43} exchange-correlation functionals, using the OPIUM⁴⁴ pseudopotential generation code.

Table V and VI list the details of the carbon and silicon pseudopotentials (PP) that were generated and tested for temperature transferability. The cut-off radius, the number of valence states and their electron occupancies were varied to study their effect on temperature dependent band gap behavior and to identify pseudopotentials that exhibit temperature transferability.

PP Name	Parameters			Band gap	
	Valence electrons	r_c (a.u.)	E_{xc}	Finite T trend	
				Indirect	Direct
C ₁	2s ² 2p ²	1.5	PBE	Decrease	Decrease
C ₂	2s ² 2p ^{1.5}	1.5	PBE	Decrease	Decrease
C ₃	2s ² 2p ¹	1.5	PBE	Decrease	Decrease
C ₄	2s ² 2p ²	1.5	PZ	Decrease	Decrease
C ₅	2s ² 2p ²	1.2	PBE	Increase	Decrease
C ₆	2s ² 2p ^{1.5}	1.2	PBE	Increase	Decrease
C ₇	2s ² 2p ¹	1.2	PBE	Increase	Decrease
C ₈	2s ² 2p ² 3d ⁰	1.5	PBE	Decrease	Decrease
C ₉	2s ² 2p ^{1.5} 3d ⁰	1.5	PBE	Decrease	Decrease
C ₁₀	2s ² 2p ¹ 3d ⁰	1.5	PBE	Decrease	Decrease
C ₁₁	2s ² 2p ² 3d ⁰	1.5	PZ	Decrease	Decrease
C ₁₂	2s ² 2p ² 3d ⁰	1.3	PBE	Inc-Dec	Decrease
C ₁₃	2s ² 2p ² 3d ⁰	1.4	PBE	Inc-Dec	Decrease
C ₁₄	2s ² 2p ² 3d ⁰	1.6	PBE	Decrease	Decrease
C ₁₅	2s ² 2p ² 3d ⁰	1.7	PBE	Decrease	Decrease

TABLE V: The trend in the indirect and direct band gap values with temperature increased up to 1000 K for the different carbon (diamond) Troullier-Martins *ab initio* pseudopotentials generated with PBE and PZ exchange correlation functional to study finite temperature behavior.

From Table V, the pseudopotentials C₁ – C₄ and C₈ – C₁₁ generated with a r_c of 1.5. a.u. showed the expected

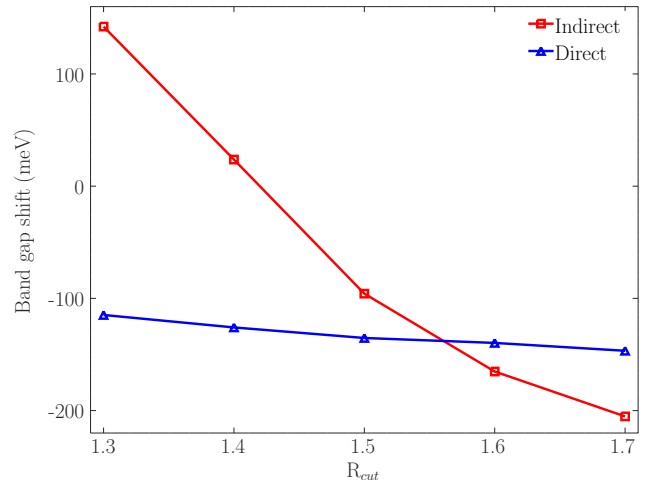


FIG. 1: Variation of zero-point band-gap shifts with cut-off radius for diamond

trend of decreasing direct and indirect band gaps with increasing temperature. However, the band gap shifts in the two sets, C₁ – C₄ and C₈ – C₁₁, differ by about 4-7 meV. We note that the pseudopotentials C₅ – C₇, that differ from C₁ – C₃ only in the cut-off radius, are not temperature transferable highlighting the sensitivity to this parameter.

To further examine the sensitivity to the cut-off radius, pseudopotentials, C₁₂ – C₁₅ were generated with cut-off radius varying from 1.3 to 1.7 a.u. From Table V it is seen that the correct trends are seen only for cut-off radius of 1.5 a.u. and above. Figure 1 plots the variation of the zero-point indirect and direct band gap shifts as a function of the cut-off radius for the carbon pseudopotentials, generated in the 2s² 2p² 3d⁰ configuration with the PBE exchange-correlation functional.

The zero-point direct band gap shift decreases weakly with the cut-off radius. This is an important result for comparison of the Allen and the Allen-Heine theories as discussed in Sec. IV B 1. In contrast, the indirect zero-point band gap shift varies strongly with the cut-off radius. The zero-point band gap shift is positive for $r_c < 1.5$ a.u. leading to an increase in the indirect band gap. Hence, carbon pseudopotentials with $r_c < 1.5$ a.u. do not exhibit temperature transferability. Only carbon pseudopotentials with $r_c > 1.5$ a.u. exhibit temperature transferability.

For silicon, from Table VI, pseudopotentials Si₈ – Si₁₀, Si_{pbe-gipaw} and Si₁₂ – Si₁₆ give the correct band gap trend with temperature. The pseudopotentials Si₁–Si₄ have the same cut-off radius (1.7 a.u.) but different valence states and their occupancies. These pseudopotentials give only the zero-point indirect band gap to be larger than that of the static lattice. For all other temperatures, the indirect band gaps decrease with increasing temperature and are smaller than that of the static lattice. In the case of the direct band gap, the zero-point band gaps are larger

than that of the static lattice. For all other temperatures, the direct band gaps decrease in comparison with the zero-point vibration gap but are higher than that of the static lattice up to temperature of 800 K.

PP Name	Parameters			Band gap	
	Valence electrons	r_c (a.u.)	E_{xc}	Finite T trend	
				Indirect	Direct
Si ₁	3s ² 3p ²	1.7	PBE	Inc-Dec	Inc-Dec
Si ₂	3s ² 3p ^{1.5}	1.7	PBE	Inc-Dec	Inc-Dec
Si ₃	3s ² 3p ¹	1.7	PBE	Inc-Dec	Inc-Dec
Si ₄	3s ² 3p ² 3d ⁰	1.7	PBE	Inc-Dec	Inc-Dec
Si ₅	3s ² 3p ²	2.0	PBE	Decrease	Inc-Dec
Si ₆	3s ² 3p ^{1.5}	2.0	PBE	Decrease	Inc-Dec
Si ₇	3s ² 3p ¹	2.0	PBE	Decrease	Inc-Dec
Si ₈	3s ² 3p ² 3d ⁰	2.0	PBE	Decrease	Decrease
Si ₉	3s ² 3p ^{1.5} 3d ⁰	2.0	PBE	Decrease	Decrease
Si ₁₀	3s ² 3p ¹ 3d ⁰	2.0	PBE	Decrease	Decrease
Si _{pbe-gipaw}	3s ² 3p ¹ 3d ⁰	2.2	PBE	Decrease	Decrease
Si ₁₂	3s ² 3p ¹ 3d ⁰	2.2	PBE	Decrease	Decrease
Si ₁₃	3s ² 3p ² 3d ⁰	1.8	PBE	Decrease	Decrease
Si ₁₄	3s ² 3p ² 3d ⁰	1.9	PBE	Decrease	Decrease
Si ₁₅	3s ² 3p ² 3d ⁰	2.1	PBE	Decrease	Decrease
Si ₁₆	3s ² 3p ² 3d ⁰	2.2	PBE	Decrease	Decrease

TABLE VI: The trend in the indirect and direct band gap values with temperature increased up to 1000 K for the different silicon Troullier-Martins *ab initio* pseudopotentials generated with PBE exchange correlation functional to study finite temperature behavior.

For the pseudopotentials Si₅-Si₇, that were generated with a cutoff radius of 2.0 a.u., the zero-point indirect band gap shows the correct behaviour i.e. smaller than the indirect band gap of the static lattice. The trend in the direct band gaps however is the same as that of Si₁-Si₄ pseudopotentials up to a temperature of 600 K. Thus, the pseudopotentials Si₁-Si₇ do not exhibit temperature transferability.

Table VI shows that the pseudopotentials Si₈-Si₁₀ differ from pseudopotentials Si₅-Si₇ in that the unbound 3d⁰ state was incorporated in the generation condition. These pseudopotentials show the correct indirect and direct band gap behavior and are hence, temperature transferable. This leads to the conclusion that incorporation of the unbound 3d⁰ state in the pseudopotential generation configuration is essential for temperature transferability of Si pseudopotentials. In addition, the pseudopotential Si₁₂ was generated with the same conditions as Si_{pbe-gipaw} except that it did not have the gipaw construction. Both Si₁₂ and Si_{pbe-gipaw} (Table IV) give virtually identical indirect and direct band gap shifts at all temperatures. This suggests that the gipaw construction does not affect temperature transferability.

To examine the dependence of the band gap shifts on the cut-off radius, pseudopotentials Si₁₃ - Si₁₆ were generated in the 3s² 3p² 3d⁰ configuration with the cut-off

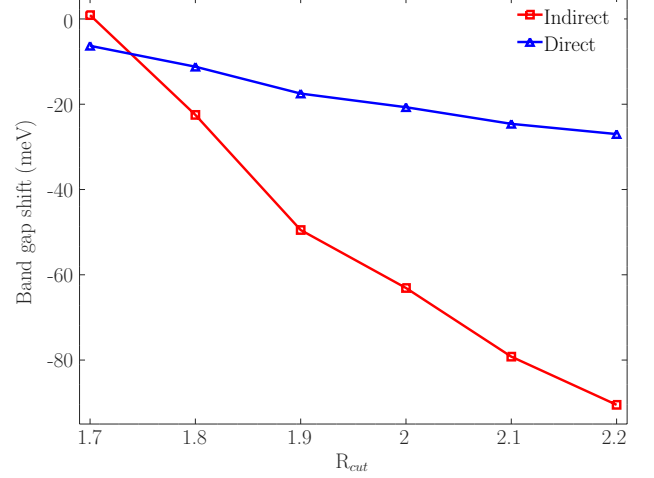


FIG. 2: Variation of zero-point band-gap shifts with cut-off radius for silicon

radius varying from 1.8 a.u. to 2.2 a.u. Figure 2 plots the zero-point indirect and direct band gap shifts as a function of the cut-off radius. It is again seen that the zero-point indirect band gap shift varies strongly with the cut-off radius. In comparison, the zero-point direct band gap shift varies much more slowly with the cut-off radius.

To summarize, the temperature transferability of Troullier-Martins pseudopotentials is dependent on the choice of the cut-off radius and the inclusion/exclusion of the unbound 3d⁰ state in the generation configuration. The cut-off radius strongly affects the indirect band gap.

These observations in combination with the usual criteria for pseudopotential generation indicate that only in a small subset of the generation parameter space of Troullier-Martins pseudopotentials the new criterion of temperature transferability is also satisfied. These observations will also be helpful in generating temperature transferable pseudopotentials for other elements that are constituents of compound semiconductors.

The question of whether other category of pseudopotentials, Optimized, Ultrasoft and ONCV pseudopotentials can also be generated to exhibit temperature transferability needs to be explored.

B. Finite temperature band structure - Diamond

We calculated the finite temperature electronic structure of diamond (a wide band gap material) at various temperatures listed in Table I from 0 – 1000 K by using the DW corrected pseudopotential form factors. While the calculations were performed for all the pseudopotentials listed in Table V, we discuss here the results obtained for pseudopotentials that exhibit the correct band gap trends.

PP	a	Band gap			
Name		Static lattice		Zero point shift	
	(a.u.)	(eV)		(meV)	
		Indirect	Direct	Indirect	Direct
C ₁	6.74	4.26	5.634	102	140
C ₂	6.73	4.28	5.635	102	142
C ₃	6.71	4.33	5.66	103	147
C ₄	6.66	4.31	5.68	107	149
C ₈	6.72	4.215	5.62	96	135
C ₉	6.71	4.247	5.64	96	138
C ₁₀	6.70	4.29	5.654	95	141
C ₁₁	6.64	4.27	5.68	100	143
C ₁₄	6.70	4.25	5.65	165	140
C ₁₅	6.68	4.29	5.67	205	146

TABLE VII: The lattice constant, indirect and direct band gaps for the static lattice and zero-point energy shifts in the direct and indirect band gaps for diamond obtained from temperature transferable pseudopotentials

Table VII gives the zero-point shifts for the pseudopotentials that exhibited temperature transferability. It shows that the zero-point band gap shifts fall into two clear sets for C₁-C₄ and C₈-C₁₁ where the former gives slightly higher shifts of 4-7 meV. All these pseudopotentials have the same cut-off radius (1.5 a.u.).

The main difference between the two sets is the incorporation of the unbound 3d⁰ state in the pseudopotential generation configuration in C₈-C₁₁. Thus, for the case of diamond, the incorporation of the unbound 3d⁰ state in the generation configuration has a consistent, but minor, effect.

The pseudopotentials C₁₄ and C₁₅ vary from C₈ only in the cut-off radius. The choice of the cut-off radius strongly influences the indirect zero-point band gap shifts. The direct zero-point band gap shifts vary weakly with the cut-off radius. Comparing with the previous results^{17,18}, based on the Allen-Heine theory, for the direct and indirect band gap shifts due to the DW term, the pseudopotentials we generated with the cut-off radius of 1.5 a.u. give the closest agreement. Hence, we restrict our discussion to the results obtained with C₈ and C₁₁ pseudopotentials that differ in the generation parameters only in the exchange-correlation functional.

For diamond, the lattice constants and the static lattice band gaps are very similar to that in previous *ab initio* studies¹⁷⁻²⁴. The band gaps are lower than the experimental values due to the well known underestimation of band gaps in density functional theory¹⁷⁻²⁴.

From Table VII it is seen that the lattice parameters for pseudopotentials with the LDA(PZ) parameterization (C₄ and C₁₁) are lower than others with the GGA(PBE) parameterization. In addition, the zero-point band gap shifts for pseudopotentials with the LDA(PZ) parameterization C₄ and C₁₁ (Table VII) are higher than others with the GGA(PBE) parameterization. Both these

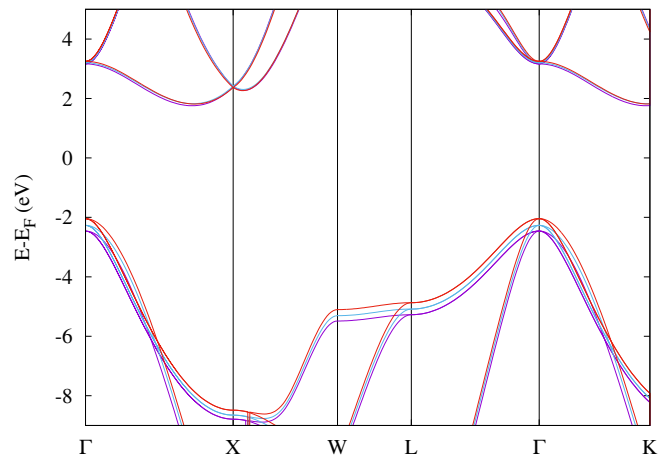


FIG. 3: The calculated band structure (static lattice and thermally-averaged) of diamond at 0 K, 300 K and 1000 K in the vicinity of the Fermi level. The violet line represents the band structure at 0 K, the blue line at 300 K and the red line at 1000 K.

trends are similar to results from previous studies¹⁸. In particular, the lattice parameter for the pseudopotential C₁₁ is 6.64 a.u. and is very similar to 3.52 Å¹⁷ and 6.652 Bohrs¹⁸ for the pseudopotential with the same generation conditions. In addition, the direct band gap for the pseudopotential C₁₁ is 5.68 eV that is very close to the value of 5.67 eV for the similar ‘reference’ pseudopotential in Ponce *et al.*¹⁸. The similarities on the lattice parameter and band gap for the pseudopotential C₁₁ with earlier results^{17,18} justifies further comparisons.

Figure 3 plots the static lattice (0 K) band structure of diamond and also the thermally-averaged band structures (at 300 K and 1000 K) for the pseudopotential C₈ for the in the vicinity of the Fermi level. The band structure is plotted so that the Fermi level at each temperature is at 0 eV. Fig. 3 demonstrates that the finite temperature thermally-averaged band structure can be obtained via an *ab initio* electronic structure calculation using *ab initio* pseudopotentials using the Allen theory formalism. The finite temperature band structures show that the valence and conduction bands shift by different amounts for different k points. From Fig. 3 it is clear that the temperature dependent band gap shifts can be obtained for any k point.

Earlier *ab initio* studies¹⁷⁻²⁴, based on the Allen-Heine theory, report the band gap shifts only at special k points, corresponding to the direct and indirect band gap shifts. The temperature dependent band structure of diamond has been obtained with path-integral molecular dynamics simulations³⁴. These simulations are computationally intensive as the ensemble-averages are calculated over $\sim 10^5$ steps³⁴. Our results highlight the advantages of implementing the Allen theory to obtain finite temperature band structures without any increase in the computational expense.

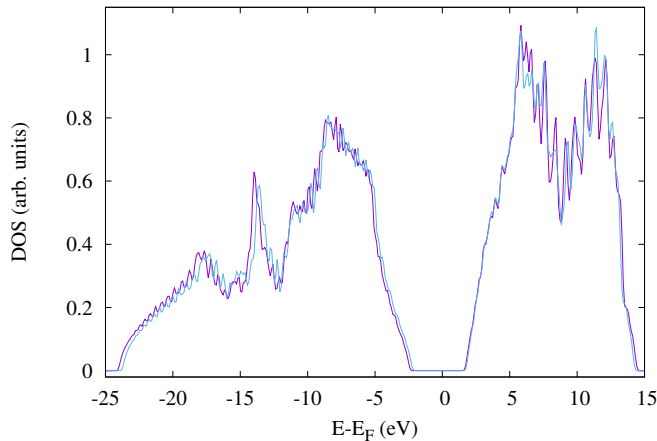


FIG. 4: The density of states of diamond at 0 K (violet) and 300 K (blue)

To understand the effect of temperature on the complete band structure we plot the density of states (DOS) for the carbon pseudopotential C_8 at 0 K and 300 K in Figure 4. The effect of temperature on the valence electron energy diagram is noticeable from the change in the DOS at 300 K. The DW term causes a positive shift of the valence electron energy levels towards the Fermi energy. The unfilled conduction band energy levels on the other hand experience a negative shift towards the Fermi energy. This feature is observed in the DOS of all finite temperature band structures that we have calculated. In the filled as well as unfilled electron energy levels, the amount of shift experienced from the static lattice is different for different levels indicating that the levels are not just scaled uniformly by a temperature dependent scaling constant.

Figure 5 plots the indirect and direct band gap shifts of diamond due to the DW term for the four carbon pseudopotentials, C_8 - C_{11} , at various temperatures. The indirect and direct band gap shifts show a non-linear behavior at low temperatures and a linear behavior at higher temperatures consistent with experimental observations²². While we have calculated the shifts for all pseudopotentials at all temperatures under investigation, we plot the results only for the pseudopotentials that exhibit good temperature transferability behavior and hence are of interest for further studies. We note that the indirect band gap shifts decrease more rapidly with temperature than the direct band gap shifts and the changes in the generation configuration, in terms of the occupancies of the 2p state, has only a minor effect at all temperatures.

1. Zero-point band gap shifts

Zero-point vibrations represent the minimum perturbation to the static lattice system. Hence, it is of interest

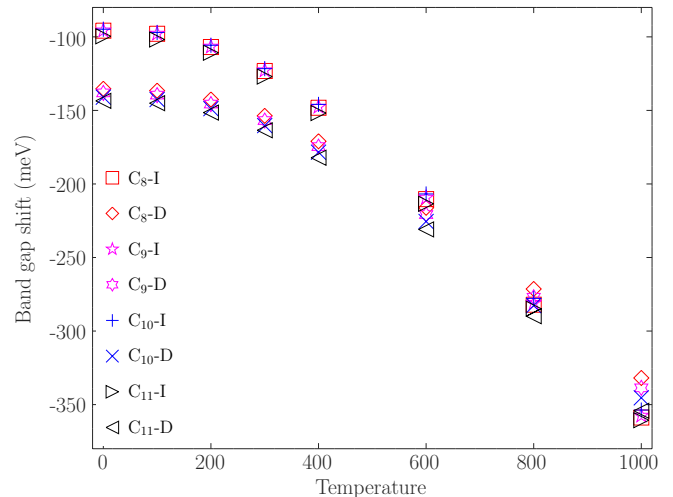


FIG. 5: The direct (D) and indirect (I) band gap shifts in diamond due to the DW term with increasing temperature for different temperature transferable carbon pseudopotentials

to examine the zero point band gap shifts in detail. For zero-point shifts, we assume that the DW term can be approximated by the second order expansion and the neglect of higher order terms in Allen-Heine theory is unimportant. That is, $V_G e^{-W} \approx V_G (1-W)$ and the Allen and Allen-Heine theories should give similar zero-point band gap shifts.

Of the several *ab initio* studies¹⁷⁻²⁴ on the band gap shifts in diamond based on Allen-Heine theory, only two^{17,18} give separately the contributions of the DW and the SE terms. Hence, the DW contribution to the zero-point shifts in our study (Table VII) can be compared with only these studies^{17,18}. In particular, our C_{11} pseudopotential has the same generation conditions as the pseudopotential in Giustino *et al.*¹⁷ and the ‘reference’ pseudopotential in Ponce *et al.*¹⁸. These studies, however, report the DW contribution only to the direct band gap and hence, the comparison is restricted to it.

The DW contribution to the direct band gap shifts for the pseudopotentials in the present study range from 135-149 meV for a variety of pseudopotential generation conditions (Table VII). In contrast, the indirect band gap shifts of these pseudopotentials (Table VII) have a much wider spread (95-205 meV) on account of the sensitivity to cut-off radius. For the direct as well as indirect band gap shifts, the pseudopotentials generated with PBE exchange correlation functional and that include the $3d^0$ state give comparatively lower shifts for a constant cut-off radius. When the direct band gap shifts are compared to the literature values^{17,18} of 105-121 meV for the zero-point shifts in the Allen-Heine theory, for Troullier-Martins pseudopotentials with a variety of generation conditions, our results are higher by about 20-30 meV.

In particular, Giustino *et al.*¹⁷ report a zero-point shift of 117 meV (19% of 615 meV) due to the DW term for

the direct band gap of diamond. Poncé *et. al.*¹⁸ report that the DW contribution ranges from 105-121 meV for four (Troullier-Martins) pseudopotentials. Of these, they report¹⁸ a direct band gap shift of 115 meV for the ‘reference’ pseudopotential, with the same generation conditions as in Giustino *et. al.*¹⁷ and in C₁₁ in the present study. This is virtually identical to the DW zero-point shift of 117 meV reported in Giustino *et. al.*¹⁷. Thus, the differences in the total (DW+SE) zero-point shifts between Giustino *et. al.*¹⁷ and Poncé *et. al.*¹⁸ is due to the SE contribution. The DW contribution to the zero-point direct band gap shift for the C₁₁ pseudopotential in the present study is 143 meV. This value can be directly compared and is ~ 26 meV higher than that reported in the above studies^{17,18}.

2. Finite temperature band gap shifts

The DW contribution to the band gap shifts calculated in the present study can also be compared with results from Allen-Heine theory at high temperatures, where the higher order terms may become important. We compare the the DW contribution to the direct band gap shifts obtained with the C₁₁ pseudopotential since it has the same generation configuration as in literature¹⁷.

Our calculated DW band gap shift of 152 meV at 200 K, 164 meV at 300 K and 231 meV at 600 K compares well with the reported DW contribution to the direct band gap shift of ~ 160 meV at 200 K, 190 meV at 300 K and 280 meV at 600K in literature¹⁷. However, an inversion must be noted. Our finite temperature DW band gap shifts are smaller while our zero-point shifts are larger compared to literature values^{17,18}.

As seen in the previous section, there is a difference of ~ 26 meV between the results obtained using the Allen and Allen-Heine theory in the DW zero-point band gap shifts. Further insight can be gained if the differences are compared with respect to the zero-point shifts which eliminates the effect of the different zero-point band gap shifts. This helps to examine the increase in the band gap shifts due to the increase in the mean-square displacements with temperature.

Eliminating the zero-point shifts, the additional DW band gap shift in our study is 9 meV at 200 K, 21 meV at 300 K and 87 meV at 600 K. These small increases in the band gap shifts with temperature can be attributed to the fact that the $\langle u_i^2 \rangle$ changes very slowly with temperature for diamond (Table I). For example, $\langle u_i^2 \rangle$ varies from 0.00161 Å² (0.001 K) to 0.00169 Å² (200 K) to 0.0018 Å² (300 K) at low temperatures.

In comparison, in Giustino *et. al.*¹⁷, after eliminating the zero-point shifts, the additional DW band gap shifts are ~ 40 meV at 200 K, 70 meV at 300 K and 160 meV at 600 K. Compared to our results above, the relatively large band gap shifts for very small increases in the mean-square displacement values (especially upto 300 K) appear excessive.

C. Silicon

Silicon, a small band gap semiconductor used extensively in a wide range of technology applications is well studied experimentally as well as theoretically and is of interest for its temperature dependent properties. We calculated the finite temperature thermally-averaged electronic structure of silicon at various temperatures listed in Table I by using the DW factor modified pseudopotential. We performed the finite temperature calculations for all pseudopotentials listed in Table VI.

Table VIII lists the zero-point shifts in the indirect and direct band gap for all the temperature transferable pseudopotentials. It shows that pseudopotentials Si₈-Si₁₀, which differ only in the valence state occupancies of p electrons, have similar zero-point shifts. The band gap shifts are virtually identical for Si_{pbe-gipaw} (Table IV) and Si₁₂ not only for zero-point vibrations but also for all other temperatures in our study. The band gap shifts increase monotonically for Si₁₃ - Si₁₆ indicating a strong dependence on the cut-off radius as seen in Figure 2.

PP Name	a (a.u.)	Band gap			
		Static lattice		Zero point shift	
		(eV)		(meV)	
		Indirect	Direct	Indirect	Direct
Si ₈	10.33	0.631	2.565	63.1	20.7
Si ₉	10.33	0.633	2.567	64.3	20.8
Si ₁₀	10.33	0.636	2.568	65.3	21
Si _{pbe-gipaw}	10.31	0.633	2.572	94	28
Si ₁₂	10.31	0.633	2.572	93	27
Si ₁₃	10.34	0.633	2.565	23	11
Si ₁₄	10.33	0.633	2.565	50	18
Si ₁₅	10.32	0.627	2.566	79	24.6
Si ₁₆	10.31	0.624	2.566	91	27

TABLE VIII: The lattice constant, indirect and direct band gaps for the static lattice and zero-point direct and indirect band gap shifts for silicon obtained from temperature transferable pseudopotentials

The static lattice direct (2.56 eV) and indirect (0.63 eV) band gaps for these pseudopotentials are very close to literature values²⁰ of 2.55 eV and 0.62 eV respectively. Si₁₂, Si_{pbe-gipaw}, Si₁₆ with higher cut-off radius have higher indirect band gap shifts and Si₁₃, Si₁₄ with a lower cut-off radius have lower band gap shifts. As observed in diamond, the indirect band gap shifts are highly sensitive to the cut-off radius used in the pseudopotentials.

Previous literature values for the total (DW + SE) shift of the indirect band gap due to zero-point vibrations are 57 meV^{20,21}, 60 meV²⁴ and 64.3 meV²² and the experimental values are 62-64 meV²¹. For the direct band gap, the reported values are 22 meV²⁰ and 47 meV²² and the experimental values are 25 ± 17 ²¹.

Previous studies^{14,15}, though based on empirical pseudopotentials, suggest that in silicon the DW term overes-

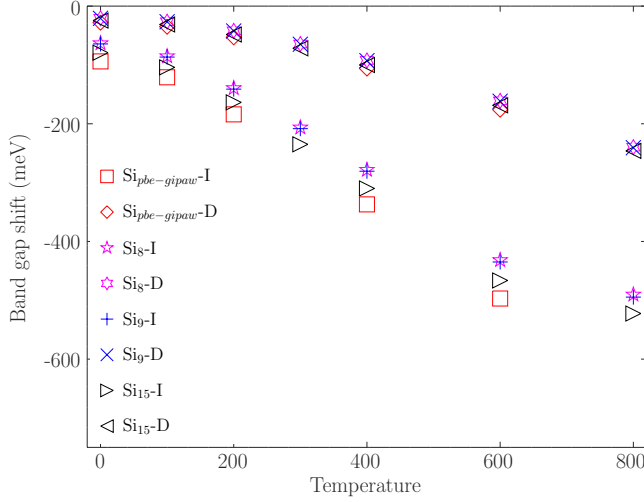


FIG. 6: The direct (D) and indirect (I) band gap shifts in silicon due to the DW term with increasing temperature for different temperature transferable pseudopotentials

timates the band gap shifts. The SE term is of opposite sign so that the total band gap shifts are less than those obtained from just the DW term.

The temperature transferable pseudopotentials in Table VIII give different magnitudes of zero-point band gap shifts than in literature^{14,15,20–22,24}. This is due to the strong sensitivity of the band gap shifts to the cut-off radius. This comparison shows that only the pseudopotentials Si₈-Si₁₀ and Si₁₅ give, band gap shifts that are the closest to previous results.

None of the *ab initio* studies on silicon separately report the DW contribution. However, Allen and Cardona¹⁴, in their study based on the Allen-Heine theory with empirical pseudopotentials, report the DW contribution to the direct band gap shift at different temperatures upto 600 K. Our DW direct band gaps shifts (Figure 6) in the temperature range upto 600 K are very similar to these reported values¹⁴. Allen and Cardona¹⁴, however, report negligible zero-point direct band gap shift, while we report a finite value.

Figure 6 plots the indirect and direct band gap shifts for the four silicon pseudopotentials, Si₈, Si₉, Si_{pbe-gipaw} and Si₁₅, at various temperatures. The indirect and direct band gap shifts exhibit a nonlinear behavior at low temperatures and a linear behavior at higher temperatures as seen in experimental studies²².

The effect of temperature on Si electronic structure is investigated and in Figure 7 we plot the (static lattice and thermally-averaged) band structure of silicon for the pseudopotential Si₈ for 0 K, 300 K and 600 K. The effect of temperature on the Si electronic structure is quite interesting with differing positive and negative shifts in the energy with respect to the static lattice. The energy shifts at the different high symmetry points in the Brillouin zone are significantly different for different temperatures. The shifts in the energy values at different points within any high symmetry line of the Brillouin zone with respect to temperature are observed to vary.

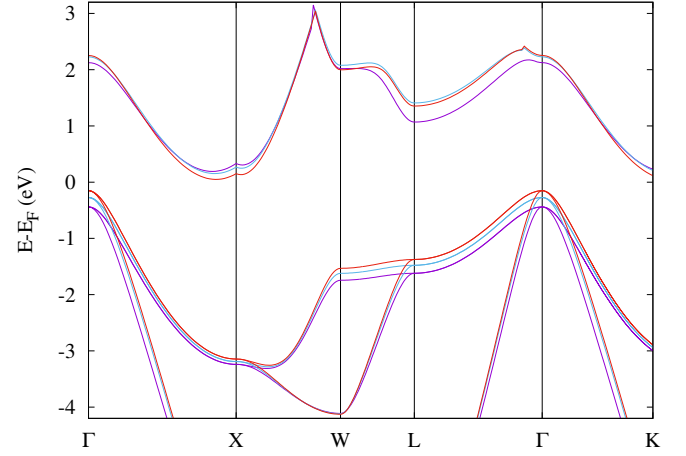


FIG. 7: The calculated band structure (static lattice and thermally-averaged) of silicon at 0K, 300K and 600K in the vicinity of the Fermi level. The violet line represents the band structure at 0 K, the blue line at 300K and the red line at 600 K.

Figure 8 plots the density of states for the silicon pseudopotential Si₈ at 0 K and 300 K. As in the case of diamond, the temperature dependent pseudopotential affects not only the valence band and conduction band energies near the Fermi level but throughout the valence and conduction bands. For finite temperatures, the filled bands and the unfilled bands shift towards the Fermi energy nonuniformly as seen in our studies on diamond. In general, the density of states broaden and shift towards the Fermi level. The amount of broadening and shift increases with increased temperature.

D. Discussion of Allen and Allen-Heine theory results

The DW term of the electron-phonon interaction is more accurately evaluated¹ in the implementation of the Allen theory, whereas, it is approximated to the second order in the Allen-Heine theory. Considering this some discrepancies in the band gap shift values obtained from these theories is expected. However, if the second-order approximation is considered to be valid, then both theories should give similar band gap shifts.

In order to separate the effect of the approximation to the DW term from other input parameters used in the calculations, it is essential that the same *ab initio* pseudopotential and mean square displacements of the atoms be used. In the present study, we have used the same pseudopotential for diamond as in previous studies^{17,18}

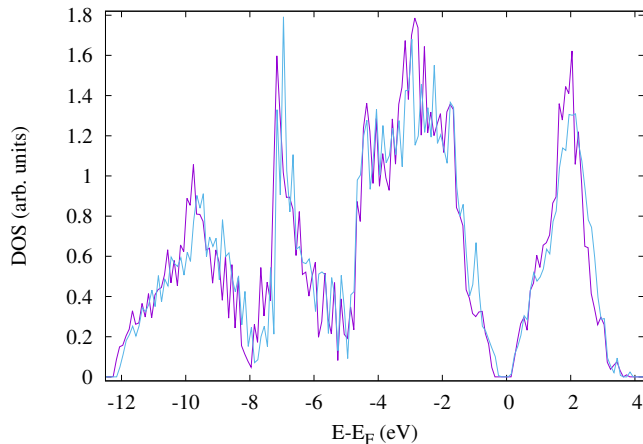


FIG. 8: The density of states of silicon at 0K (violet) and 300K (green)

based on the Allen-Heine theory. The mean square displacement values as in previous studies however, could not be used since they have not been reported.

The implementation of Allen theory is based on using explicit values of the mean-square displacements, whereas in the Allen-Heine theory the mean-square displacement values are not directly used and are implicit. In our study of finite temperature properties of diamond and silicon explicit values of the mean-square displacements obtained from *ab initio* studies have been used. If the values of the mean-square displacements are different from that in the earlier studies, then discrepancies can be expected in the results from the two theories.

In the case of diamond, we have used (Table I) the zero-point mean-square displacement values reported in Schowalter *et al.*²⁶. A similar value, for the zero-point vibrations, has also been reported in Yang *et al.*²⁷. In both these studies^{26,27}, the mean-square displacement values have been obtained from density-functional perturbation theory. The previous Allen-Heine based studies^{17,18} that reported the DW contribution to the direct band gap shift also use the density-functional perturbation theory to account for thermal vibrations, though explicit values of the zero-point mean-square displacements are not reported. Since there are some discrepancies in the DW band gap shifts for diamond (as seen earlier), it would be of interest to compare the zero-point mean-square displacements implicit in the Allen-Heine theory based studies^{17,18} with the explicit values reported in literature^{26,27} that are used in our study based on the Allen theory.

If the mean-square displacement values used in the two theories are the same, then the discrepancies, if any, are likely due to the different numerical implementations of the electron-phonon contribution to the electronic energies in the two theories.

Clearly, further studies are needed to fully understand

the results obtained using the Allen and Allen-Heine theories. Such studies for any semiconductor, however must necessarily use temperature transferable pseudopotentials.

E. Finite temperature valence charge density

Finite temperature charge densities are of interest, both theoretically and experimentally, to study bonding in materials. At present, there is no simple *ab initio* method to obtain finite temperature valence electron wavefunctions or charge densities. Currently, finite temperature charge densities are obtained from static lattice calculations with empirical approaches to incorporate the effect of thermal vibrations as discussed below.

The valence electron densities have been experimentally obtained for several materials from x-ray diffraction and electron diffraction studies^{45–50}. In particular, silicon and diamond are considered to be the prototype materials in experimental (valence) electron density studies^{45,46}. In these studies, the ‘fundamental step’⁴⁶ is to correct for the observed intensities at finite temperatures with the DW factor^{45–50}. Following this correction, an effective static lattice charge density is obtained. Subsequently, these charge densities are compared with theoretical *ab initio* calculations performed for static lattice^{45–48}.

Alternately, the theoretical charge density from static lattice calculations are altered by incorporating thermal vibrations through the DW factors and the finite temperature charge densities or structure factors so obtained are compared with finite temperature experimental values^{49,50}.

Fundamental to these approaches is the assumption of the rigid pseudo-atom approximation^{51,52}, viz. the electron density, including the valence electron density, can be partitioned to individual atoms and each such segment is frozen and moves rigidly with the thermal vibrations. This leads to the DW factor correction, the ‘fundamental step’ in the charge density studies. We note that Jones and March⁵² had raised concerns about the validity of the rigid pseudo-atom approximation for valence electrons.

In the rigid pseudo-atom approximation, since the valence charge densities move rigidly with thermal motion, it implies that there is no change in the valence electron wavefunctions and energies. It follows that the band gaps must be unchanged with temperature. This is contrary to experimental and theoretical observations^{4,5,14–24}. This is a simple demonstration of the incorrectness of the rigid pseudo-atom approximation for valence electrons in silicon and diamond. Hence, at present, there is no simple and theoretically justified method to obtain finite temperature valence charge densities.

In the Allen theory², the first step is to include the DW term in the pseudopotential form factor (Eq. 6) and then calculate the electronic structure. That is, the wavefunctions and charge densities of valence electrons so ob-

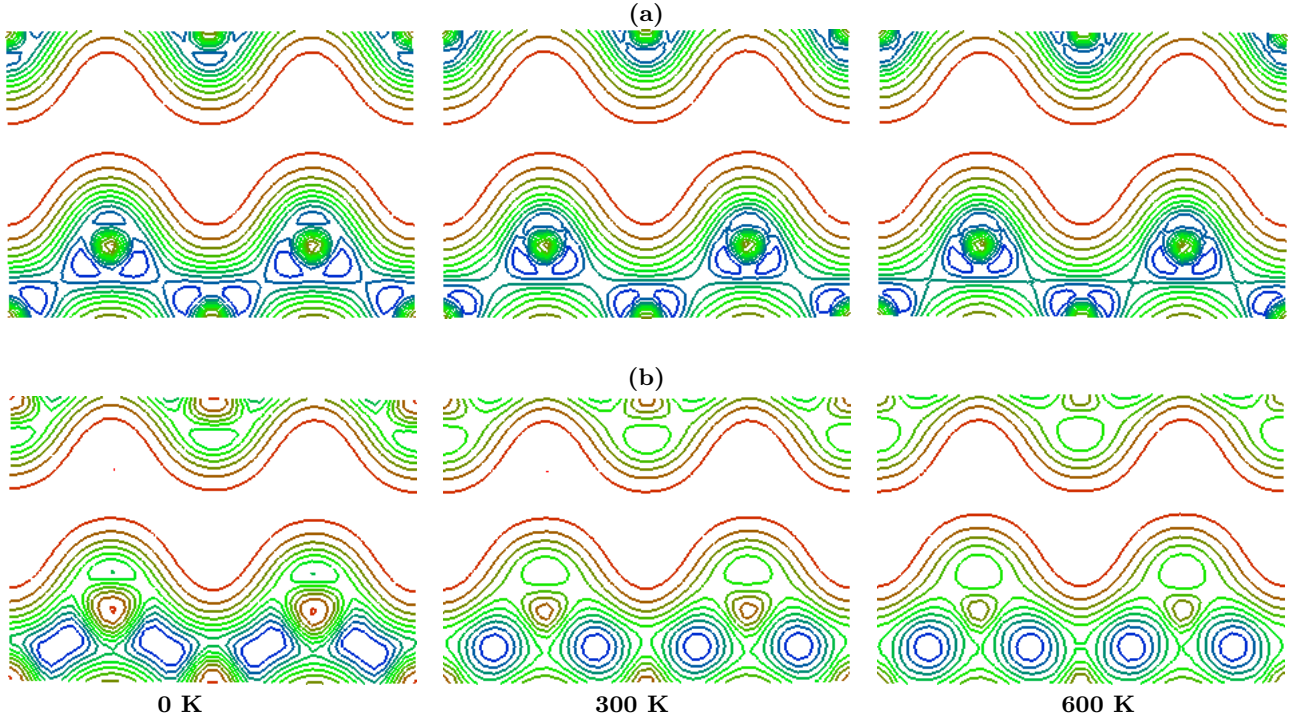


FIG. 9: The charge density along the (110) plane for (a) diamond and (b) silicon. The charge density of the static lattice (0 K) is shown in the left panel, at 300 K in the middle panel and at 600 K in the right panel for both the materials

tained are temperature dependent and not frozen. Thus, the Allen theory provides a simple way to go beyond the rigid pseudo-atom approximation to theoretically obtain finite temperature valence charge densities.

Further, in the Allen theory², the SE corrections to the electron energies are calculated from the results of the above step. That is, there is no further correction of the wavefunctions. Hence, the first (DW) step of the Allen theory is sufficient to obtain finite temperature valence charge densities.

Figure 9 plots the (pseudo) valence charge densities of (a) diamond (C_8) and (b) silicon (Si_8) at 0 K, 300 K and 600 K. It shows that the charge distribution in the bonding region is enhanced with an increase in temperature. In general, the charge delocalization in silicon increases with increasing temperature. It is interesting to note that the differences in the charge density distribution at 300 K and 600 K compared to that at 0 K are more for silicon than diamond. This is due to the much higher mean square displacements of silicon compared to diamond (Table I). In silicon, the charge density distribution at finite temperatures shows more accumulation of charges in the bonding region with a reduction in the charge density in the vicinity of the core region. With better exchange correlation functionals, which reduce the underestimation of the band gaps, a more accurate charge density distribution would be obtained. In diamond, a similar effect is observed with a minor gain in the charge densities in the covalent bonding region.

As is well known^{53,54}, the pseudopotential method only

gives pseudo-valence charge densities. They are incorrect near the nuclei. However, away from the nuclei and in the valence region, the pseudo-valence charge densities are similar to the true valence charge densities^{53,54}. The finite temperature charge density information in the valence region is valuable as this is the region where bonding effects are strongly manifested. The pseudo-valence charge densities plotted in Fig. 9 thus go beyond the rigid pseudo-atom approximation. Therefore, if the experimental data can also be analyzed appropriately to obtain finite temperature experimental charge densities, they can be compared with the theoretical results obtained from the Allen theory, a comparison that goes beyond the rigid pseudo-atom approximation.

V. CONCLUSIONS

In this paper, we report the implementation of the Allen theory with *ab initio* pseudopotentials in density functional total energy calculations to obtain the finite temperature thermally-averaged electronic structure without any additional increase in the computational complexity and cost. Our results on diamond and silicon show that both the direct and indirect band gaps exhibit the “Varshni effect” with temperature only when the *ab initio* pseudopotentials satisfy an additional criterion, that of temperature transferability. The temperature transferability criterion is satisfied only in a small subset of the parameter space of static lattice in

Troullier-Martins pseudopotentials for diamond and silicon. In these materials, the temperature transferability is strongly affected by the choice of the cut-off radius and inclusion/exclusion of unbound $3d^0$ state in the pseudopotential generation configuration. The finite temperature indirect band gaps in diamond and silicon are seen to be highly sensitive to the choice of cut-off radius.

Our results on finite temperature electronic structure show that the thermal vibrations affect the electron energies throughout the valence and conduction bands. We have calculated the zero-point and higher temperature band gap shifts in diamond and silicon for temperatures up to 1000 K. We compared our results on direct band gap shifts with those obtained using the Allen-Heine theory for the contribution from the Debye-Waller term. For diamond, our zero-point shifts in the direct band gaps are higher by 26 meV for the same *ab initio* pseudopotentials. The finite temperature direct band gap shifts also show noticeable discrepancies. For silicon, we see a good agreement in the band gap shifts with the only results reported in literature (for the DW contribution) using empirical pseudopotentials. Further studies using the same temperature transferable *ab initio* pseudopotentials and

mean square displacements are essential to understand the discrepancies in the Allen and Allen-Heine theory band gap shifts, especially since the former, besides being more accurate, has a simpler numerical implementation.

The inclusion of Debye-Waller correction using the Allen theory provides a simple and theoretically justified formalism to obtain finite temperature valence electron charge densities. The finite temperature charge densities obtained using Allen theory go beyond the rigid pseudopotential approximation, a limitation of the present methods used in charge density studies.

VI. ACKNOWLEDGEMENT

V.S. acknowledges funding support under the DST Nanomission, DST PURSE, DRDP and BCUD research grant from Savitribai Phule Pune University. B.S. and R.R. acknowledge helpful discussions with Aditya Vishwakarma and Harshit Bharti on the use of OPIUM software.

-
- ¹ P. B. Allen and V. Heine, J. Phys. C **9**, 2305 (1976).
 - ² P. B. Allen, Phys. Rev. B **18**, 5217 (1978).
 - ³ P. B. Allen and J. C. K. Hui, Z. Phys. B **37**, 33 (1980).
 - ⁴ F. Giustino, Rev. Mod. Phys. **89**, 015003 (2017).
 - ⁵ S. Poncé, G. Antonius, Y. Gillet, P. Boulanger, J. L. Janssen, A. Marini, M. Côté, and X. Gonze, Phys. Rev. B **90**, 214304 (2014).
 - ⁶ H. Y. Fan, Phys. Rev. **82**, 900 (1951).
 - ⁷ E. Antončík, Czech. J. Phys. **5**, 449 (1955).
 - ⁸ C. Keffer, T. M. Hayes, and A. Bienenstock, Phys. Rev. Lett. **21**, 1676 (1968).
 - ⁹ J. P. Walter, R. R. Zucca, M. L. Cohen, and Y. Shen, Phys. Rev. Lett. **24**, 102 (1970).
 - ¹⁰ R. Kasowski, Phys. Rev. B **8**, 1378 (1973).
 - ¹¹ M. Schlüter, G. Martinez, and M. L. Cohen, Phys. Rev. B **12**, 650 (1975).
 - ¹² M. Cardona and M. Thewalt, Rev. Mod. Phys. **77**, 1173 (2005).
 - ¹³ K. Baumann, Physica Status Solidi (b) **63**, K71 (1974).
 - ¹⁴ P. B. Allen and M. Cardona, Phys. Rev. B **27**, 4760 (1983).
 - ¹⁵ S. Zollner, M. Cardona, and S. Gopalan, Phys. Rev. B **45**, 3376 (1992).
 - ¹⁶ A. Marini, Phys. Rev. Lett. **101**, 106405 (2008).
 - ¹⁷ F. Giustino, S. G. Louie, and M. L. Cohen, Phys. Rev. Lett. **105**, 265501 (2010).
 - ¹⁸ S. Poncé, G. Antonius, P. Boulanger, E. Cannuccia, A. Marini, M. Côté, and X. Gonze, Comput. Mater. Sci. **83**, 341 (2014).
 - ¹⁹ G. Antonius, S. Poncé, P. Boulanger, M. Côté, and X. Gonze, Phys. Rev. Lett. **112**, 215501 (2014).
 - ²⁰ C. E. Patrick and F. Giustino, J. Phys. Condens. Matter **26**, 365503 (2014).
 - ²¹ M. Zacharias and F. Giustino, Phys. Rev. B **94**, 075125 (2016).
 - ²² S. Poncé, Y. Gillet, J. Laflamme Janssen, A. Marini, M. Verstraete, and X. Gonze, J. Chem. Phys. **143**, 102813 (2015).
 - ²³ B. Monserrat, N. Drummond, and R. Needs, Phys. Rev. B **87**, 144302 (2013).
 - ²⁴ B. Monserrat and R. Needs, Phys. Rev. B **89**, 214304 (2014).
 - ²⁵ J. C. Slater, *Quantum Theory of Molecules and Solids*, vol. 3 (McGraw-Hill New York, 1967).
 - ²⁶ M. Schowalter, A. Rosenauer, J. Titantah, and D. Lamoén, Acta Crystallogr. Sec. A **65**, 5 (2009).
 - ²⁷ Y. Yang and Y. Kawazoe, Europhys. Lett. **98**, 66007 (2012).
 - ²⁸ A. Erba, M. Ferrabone, R. Orlando, and R. Dovesi, J. Comput. Chem. **34**, 346 (2013).
 - ²⁹ C. Pisani, A. Erba, M. Ferrabone, and R. Dovesi, J. Chem. Phys. **137**, 044114 (2012).
 - ³⁰ F. Vila, V. Lindahl, and J. Rehr, Phys. Rev. B **85**, 024303 (2012).
 - ³¹ S. Baroni, S. de Gironcoli, A. Dal Corso, and P. Giannozzi, Rev. Mod. Phys. **73**, 515 (2001).
 - ³² K. Parlinski, Z. Li, and Y. Kawazoe, Phys. Rev. Lett. **78**, 4063 (1997).
 - ³³ H. Neumann, J. Łażewski, P. Jochym, and K. Parlinski, Phys. Rev. B **75**, 224301 (2007).
 - ³⁴ R. Ramírez, C. P. Herrero, and E. R. Hernández, Phys. Rev. B **73**, 245202 (2006).
 - ³⁵ P. Giannozzi, S. Baroni, N. Bonini, M. Calandra, R. Car, C. Cavazzoni, D. Ceresoli, G. L. Chiarotti, M. Cococcioni, I. Dabo, et al., J. Phys. Condens. Matter **21**, 395502 (2009).
 - ³⁶ M. Schlipf and F. Gygi, Comput. Phys. Commun. **196**, 36 (2015).
 - ³⁷ K. F. Garrity, J. W. Bennett, K. M. Rabe, and D. Vander-

- bilt, Comput. Mater. Sci. **81**, 446 (2014).
- ³⁸ *Virtual vault for pseudopotentials and paw datasets*, URL <http://nninc.cnf.cornell.edu/>.
- ³⁹ Y. P. Varshni, Physica **34**, 149 (1967).
- ⁴⁰ N. Troullier and J. L. Martins, Phys. Rev. B **43**, 1993 (1991).
- ⁴¹ J. Perdew, K. Burke, and M. Ernzerhof, Phys. Rev. Lett. **77**, 3865 (1996).
- ⁴² D. M. Ceperley and B. Alder, Phys. Rev. Lett. **45**, 566 (1980).
- ⁴³ J. P. Perdew and A. Zunger, Phys. Rev. B **23**, 5048 (1981).
- ⁴⁴ *Opium pseudopotential generation project*, URL <http://opium.sourceforge.net>.
- ⁴⁵ N. Bindzus, T. Straasø, N. Wahlberg, J. Becker, L. Bjerg, N. Lock, A.-C. Dippel, and B. B. Iversen, Acta Crystallogr. Sec. A **70**, 39 (2014).
- ⁴⁶ N. Wahlberg, N. Bindzus, L. Bjerg, J. Becker, A.-C. Dippel, and B. B. Iversen, Acta Crystallogr. Sec. A **72**, 28 (2016).
- ⁴⁷ P. N. Nakashima, A. E. Smith, J. Etheridge, and B. C. Muddle, Science **331**, 1583 (2011).
- ⁴⁸ X. Sang, A. Kulovits, G. Wang, and J. Wieszorek, Philos. Mag. **92**, 4408 (2012).
- ⁴⁹ J. Zuo, M. O'keeffe, P. Rez, and J. Spence, Phys. Rev. Lett. **78**, 4777 (1997).
- ⁵⁰ S. Dudarev, L.-M. Peng, S. Savrasov, and J.-M. Zuo, Phys. Rev. B **61**, 2506 (2000).
- ⁵¹ C. Gatti and P. Macchi, *Modern Charge-Density Analysis* (Springer Science & Business Media, 2012).
- ⁵² W. Jones and N. March, *Theoretical Solid State Physics, Volume 1: Perfect Lattices in Equilibrium* (Wiley Interscience, 1973).
- ⁵³ Z. Lu, A. Zunger, and M. Deutsch, Phys. Rev. B **47**, 9385 (1993).
- ⁵⁴ M. Yin and M. L. Cohen, Phys. Rev. B **26**, 5668 (1982).